



a free-access multidisciplinary publication
of the Faculty of Engineering Hunedoara

1. Konstantinos-Dionysios BOUZAKIS, 2. Georgios SKORDARIS,
3. Emmanouil BOUZAKIS, 4. Nikolaos MICHAILIDIS

CHARACTERIZATION METHODS AND PERFORMANCE OPTIMIZATION OF COATED CUTTING TOOLS

^{1,4} Aristoteles University of Thessaliniki, Fraunhofer Project Center Coatings in Manufacturing (PCCM), Thessaloniki, GREECE

Abstract: Coated tools constitute the majority of the tools applied in material removal processes. Analytical-experimental methodologies for predicting film properties and cutting performance of coated tools are introduced. Stress-strain curves and fatigue critical loads of coatings are determined at various temperatures by nanoindentations and impact tests respectively. The film adhesion is assessed effectively by inclined impact tests and the film brittleness by nano-impacts. The effect of the cutting edge impact duration in milling on the tool performance is captured via impact tests at various force signal times. Moreover, micro-blasting on PVD coatings at appropriate conditions improves the coated tool life. The relevant results are evaluated by Finite Elements Method (FEM) procedures. The described procedures allow the prediction of coated tool cutting performance and the effective adaption of the cutting conditions to the film properties, thus restricting the related experimental cost.

Keywords: PVD films, strength properties, fatigue, adhesion, brittleness, cutting edge entry impact duration, micro-blasting, milling

1. INTRODUCTION

Coated tools have compound material structure, consisting of the substrate covered with a hard, anti-friction, chemically inert and thermal isolating layer, approximately one to few micrometers thick. As such, coated tools compared to uncoated ones, offer better protection against mechanical and thermal loads, diminish friction and interactions between tool and chip and improve wear resistance in a wide cutting temperature range [1].

| PROPERTIES | | TEST METHODS | | | | | | | | | | | | | | | | | |
|--------------------|--|--------------|-----|-----|-----|----|----|-----|----|-------|----|-----|-----|---|----|----|-----|----|-----|
| | | EDX | SEM | XRD | TEM | .. | NI | NIT | IT | ITMFS | BC | WLS | IIT | S | NS | RC | DIF | OX | TRM |
| Material | Structure | √ | √ | √ | | | | | | | | | | | | | | | |
| | Residual stresses | | | √ | | | | | | | | | | | | | | | |
| | Mechanical properties | | | | | | √ | | | | | | | | | | | | |
| | Hardness | | | | | | √ | | | | | | | | | | | | |
| | Brittleness | | | | | | | √ | | | | | | | | | | | |
| Dimensional | Fatigue | | | | | | | √ | | | | | | | | | | | |
| | Fatigue at high strain rates | | | | | | | | √ | | | | | | | | | | |
| | Thickness | | | | | | | | | √ | | | | | | | | | |
| Functional | Thickness distribution on the cutting edge | | | | | | | | | | √ | | | | | | | | |
| | Friction | | | | | | | | | | | | | | | | | | √ |
| | Adhesion | | | | | | | | | | | √ | √ | √ | √ | | | | |
| | Diffusion | | | | | | | | | | | | | | | | √ | | |
| Chemical stability | Chemical stability | | | | | | | | | | | | | | | | | | √ |

Figure 1. Characteristic methods for determining coating material, dimensional and functional properties. The cutting performance of coated tools can be significantly improved by tailoring the coatings properties to application specific requirements. For achieving this target, a thorough

understanding of the coated tools wear mechanisms is required [2]. Since PVD thin films are very hard and brittle materials, properties such as fatigue, toughness, residual stresses and adhesion along with tribological and dimensional ones are pivotal for cutting with coated tools. To quantify these parameters, experimental-analytical test procedures have been developed (see figure 1). These provide information concerning material and functional properties of the film and its substrate as well as the actual coated tool geometry. Combinations of these procedures jointly with FEM supported computations contribute to the explanation of the cutting tool films' failure mechanisms, thus restricting the experimental cost for optimizing cutting conditions. Moreover, coating mechanical treatment such of micro-blasting can contribute to cutting performance improvement by adjusting appropriately the micro-blasting conditions.

2. STRENGTH AND FATIGUE PROPERTIES AT AMBIENT AND ELEVATED TEMPERATURES DETERMINED BY NANOINDENTATIONS AND IMPACT TESTS

The determination of coating strength properties and hardness is conducted by nanoindentations [3,4,5]. Nanoindentations at elevated temperatures facilitate the estimation of temperature dependent film strength properties [6,7,8,9]. This technique enables in "situ" measurements, thus yielding to an accurate determination of coating properties in a wide range of temperatures.

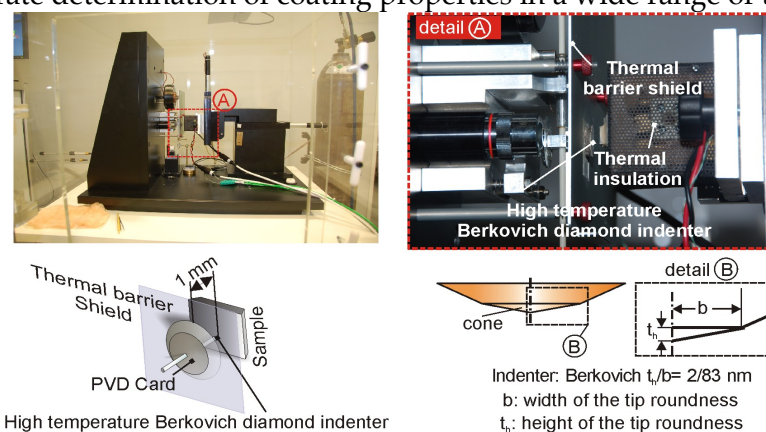


Figure 2. Experimental set up for nanoindentations at ambient and elevated temperatures

In figure 2, Micro Materials Ltd instrument to conduct nanoindentation measurements at elevated temperatures is shown. Nanoindentations up to 600°C can be conducted, employing various indenters; both indenter and specimen are heated. To avoid oxidations, the measurements are conducted in an inert atmosphere. The contact between the sample and the indenter is schematically shown at the bottom figure part. The precise mathematical description of the equivalent tip geometry of a Berkovich indenter is facilitated, employing developed methods documented in the literature [3].

Characteristic nanoindentation measurements on a TiAlN coating, at various temperatures up to 400°C, are exhibited in figure 3a [9]. Each curve represents a mean value of 50 measurements. After approximately twenty measurements, the moving average of the maximum penetration depth is stabilized [3]. According to these results, the registered maximum indentation depth depends on the film temperature. The maximum indentation depth at a temperature of about 150°C is lower than the corresponding one at ambient temperature. At larger temperatures, the indentation depth (ID) growth at approximately 300°C is followed by an ID reduction at ca. 400°C, however more restricted compared to the corresponding one at 150°C. Employing the "SSCUBONI" algorithm, the film's stress-strain curves at various temperatures are calculated (see figure 3b). According to these results, the film elasticity modulus remains unaffected by the temperature increase up to 400°C. Moreover, a significant growth of yield and rupture stress at 150°C and at 400°C develops. The film yield stress and the rupture stress course versus the temperature are presented in figure 3c.

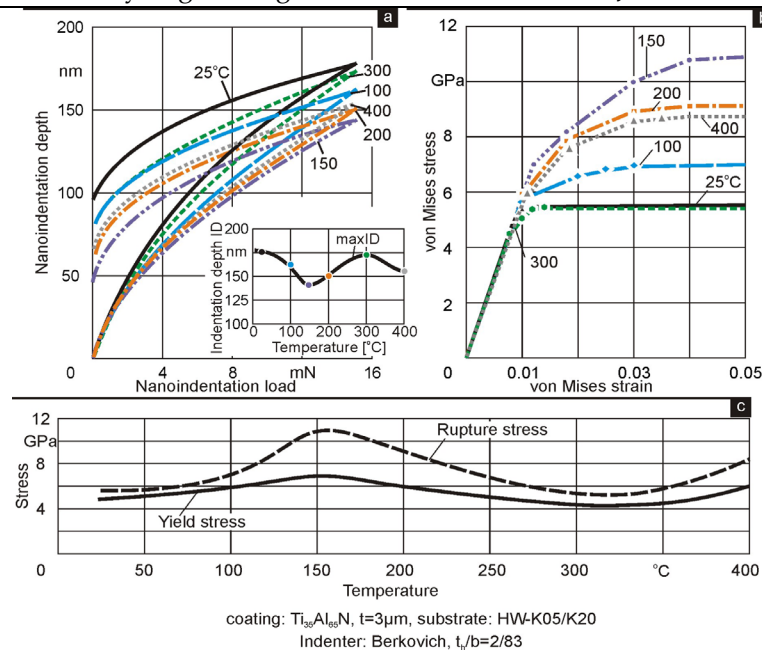


Figure 3. (a) Nanoindentation diagrams of a TiAlN coating at various temperatures. (b) Calculated stress – strain curves the applied TiAlN coating at various temperatures. (c) Correlation between yield and fatigue endurance stress of a TiAlN coating at various temperatures.

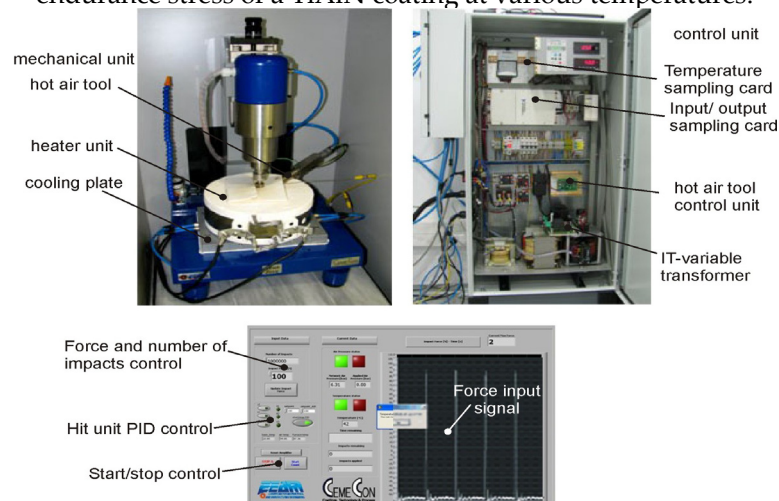


Figure 4. Experimental set up for nanoindentations at ambient and elevated temperatures. Films' fatigue properties at ambient and elevated temperatures are determined by perpendicular impact tests, employing an appropriate device (see figure 4) [1,9,10]. This device was developed and manufactured by the Laboratory for Machine Tools and Manufacturing Engineering of the Aristoteles University of Thessaloniki in conjunction with CemeCon AG. A new heating module was developed and implemented in the Impact Tester (IT) experimental setup. A high-efficiency heater and hot air tool were integrated in the existing impact tester setup, capable of raising the test temperature over 400°C (see figure 4). The power unit was upgraded to facilitate the integration of several new functions, safety sensors and controls. The operation of the heating module is controlled and monitored by suitably developed computer software, integrated into the existing IT control. The test temperature is kept constant by means of PID control, ensuring temperature stability, safe operation and the reliability of the obtained results. Moreover, in order to avoid the overheating of the impact tester's structural parts and its sensitive instruments and to minimize thermal energy dissipation, a cooling system through pressed air is applied in conjunction with suitable thermal insulation.

The wear propagation of a PVD HIS TiAlN coating during the impact test at temperatures up to 400°C is monitored in terms of the coating fracture ratio (FR) versus the applied impact force F in figure 5a [9]. Each plotted point corresponds to a test duration of 10^6 impacts. The profile of the

coating FR, under various operational temperatures, captures the coating removal rate versus the impact force. The worst performance appears at 300°C and the overall best, at a temperature of 150°C. At this temperature level, the coating withstands up to almost 140 daN before being totally removed (FR=100%) after 10⁶ impacts. SEM micrographs of the impressions related to various test loads, just before the coating failure start (FR<3%), are illustrated in figure 5b.

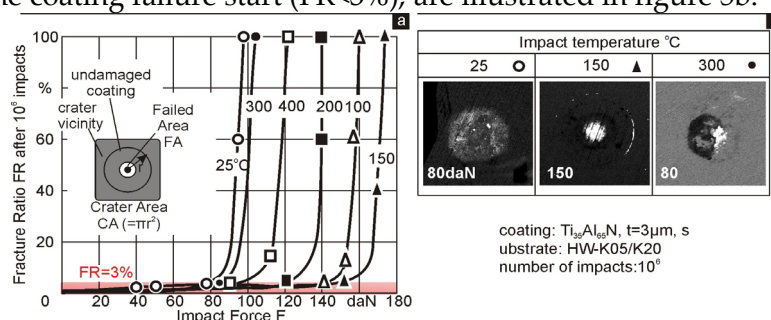


Figure 5. (a) Coating fracture ratios after 10⁶ impacts at various temperatures and load. (b) SEM micrographs of the impact imprints

Considering the FEM calculated temperature fields during milling at various cutting speeds, a correlation between the coating impact resistance at different temperatures to the tool wear results at various cutting speeds were attained [11]. The critical force after 10⁶ impacts at a coating fracture ratio less than 3% and the number of the cuts in milling versus the cutting speed and the impact test temperature, up to a flank wear of 0.2 mm, are exhibited in figure 6. The recorded impact test temperatures according to the conducted FEM calculations correspond to the cutting speeds, as displayed in this figure. Considering these results, the coating cutting performance versus the cutting speed correlates with the impact resistance versus the temperature. The possibility to calculate cutting temperatures on the tool surface and to correspond them to coatings' mechanical properties, as shown in figure 6, allows the prediction of the cutting speed regions associated with improved coated tools cutting performance.

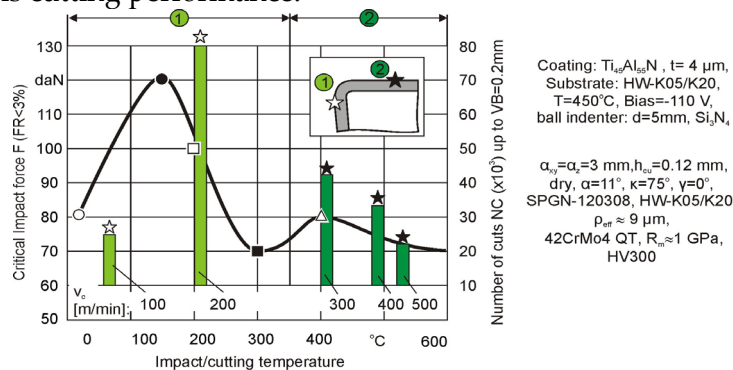


Figure 6. Correlation between the cutting performance and the coating impact resistance

3. INCLINED IMPACT TEST FOR ASSESSING FILM ADHESION QUALITY

The film adhesion can be characterized by Rockwell test [12], inclined impact test [13] and in the case of thin films (<0.5 μm) by nano-scratch test [14]. It has to be pointed out that the Rockwell test for investigating the film adhesion in some cases is insufficient. For example, for testing the effect of HPPMS graded Cr/CrN-interlayer thickness on the film adhesion [15], Rockwell HRC indentations were conducted on the coated inserts. The Rockwell imprints were captured by confocal measurements and are monitored in Figure 7a. No cracks or detachments appear in the imprints vicinity of the coated inserts with graded Cr/CrN-interlayers of different thicknesses. According to these results, the adhesion may be characterized as good, in all coating cases.

Furthermore, the wear resistance of HPPMS TiAlN coated inserts with graded Cr/CrN-interlayer of various thicknesses was checked in milling using a numerically controlled 3D milling center, by programming circular paths around cylindrical workpieces without the usage of coolant or lubricant (see figure 7b). According to the obtained results, the coated inserts with graded Cr/CrN-

nanointerlayer thickness of 200 nm exhibit the best wear resistance, reaching a tool life of approximately 140.000 cuts, at a flank wear width VB of 0.2 mm. Moreover, coated inserts with 50 nm and 600 nm nanointerlayer managed to cut only ca. 100.000 and 90.000 times respectively, up to the flank wear width of 0.2 mm.

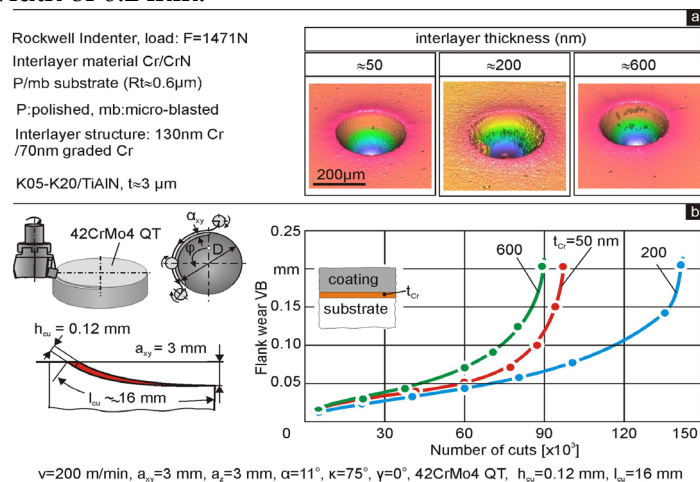


Figure 7. (a) Rockwell C indentation imprints on the examined coated inserts with various HPPMS deposited Cr/CrN adhesive interlayers' thicknesses. (b) Flank wear development versus the number of cuts of coated tools with different Cr/CrN interlayer thickness.

The cutting performance deterioration, when the adhesive interlayer thickness amounts to 50 or 600 nm can be attributed to the coating adhesion diminution [15]. Due to the perpendicular loading direction during the Rockwell indentation, the thin layers are pressed against the substrate, i.e. no shear loads within the interlayer occur, which can lead to shear fracture. In this way, no detachments or cracks develop, i.e. a good adhesion is concluded. On the other hand, the oblique loading direction during the inclined impact test can cause the shear fracture of interlayers. Thus, to examine the coating adhesion, compressive and shear loads have to be simultaneously exercised. The inclined impact test renders possible the exercise of such loads on the film surfaces.

This can be also validated by the developed FEM determined equivalent stresses at various contact stiffness ratio during the inclined and the perpendicular impact test [13]. The ratio CSR of the tangential contact stiffness c_{st} , to the normal one c_{sn} , is applied to characterize the adhesion strength in the coating-substrate region [13]. As can be seen in figure 8, the contact stiffness ratio has no effect on the developed maximum equivalent stress in the perpendicular impact test. Furthermore, during the inclined impact test, the decrease of the contact stiffness ratio, i.e. the film adhesion deterioration, results in a nonlinear growth of the maximum equivalent stress. The stress augmentation is more intensive as the coated surface inclination angle increases. These results indicate that at the same impact force, the film adhesion affects the developed maximum stress during the inclined impact test and therefore the film damage.

By inclined impact tests [15], significant adhesion differences can be detected. The removed film volume ratios (RVR) versus the number of impacts on the examined inserts with various interlayers thicknesses were determined by inclined impact tests and they are exhibited in left part of figure 9a. The TiAlN coated inserts with graded Cr/CrN-interlayers of 200 nm withstand more effectively the repetitive oblique impact loads compared to the corresponding interlayers of 50 and 600 nm thicknesses. In milling investigations, applying the HPPMS TiAlN coated inserts with graded Cr/CrN-interlayer of various thicknesses (see right part of figure 9a), the cutting performance can be correlated to the oblique impact resistance during the inclined impact tests. This is also visible in Figure 9b, where the number of impacts up to a removed film volume ratio of 10% and the number of cuts up to flank wear width of 0.15 mm of HPPMS TiAlN coated inserts with various graded Cr/CrN-nanointerlayer thicknesses appear the same tendency.

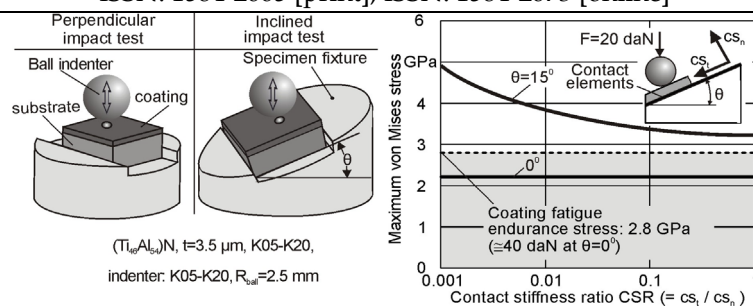


Figure 8. Effect of the contact stiffness ratio on the occurring maximum equivalent stress during the inclined and the perpendicular impact test.

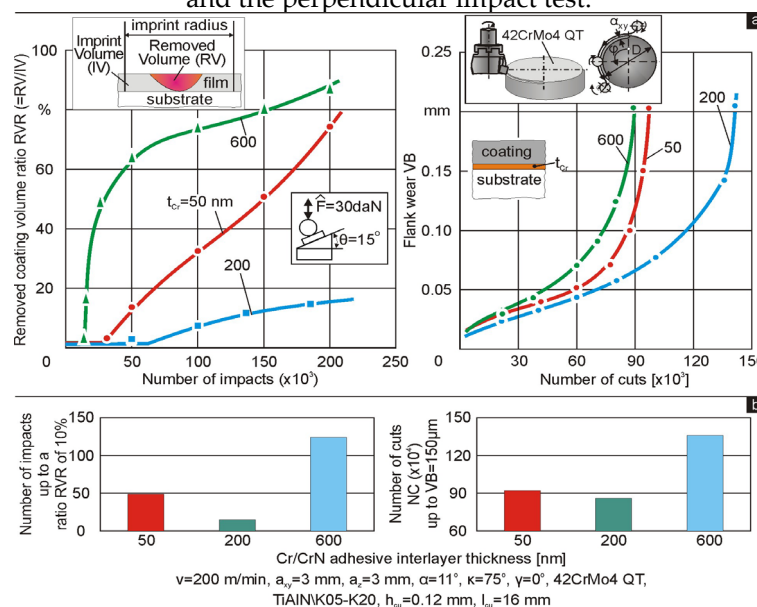


Figure 9. (a) Effect of HPPMS interlayers' thickness on the removed coating volume during the inclined impact test of coated inserts and flank wear development versus the number of cuts of coated tools with different interlayer thickness. (b) Number of impacts up to a ratio RVR of 10% and number of cuts up to VB=0.15 of coated inserts with various HPPMS deposited Cr/CrN adhesive interlayers' thicknesses.

4. NANO-IMPACT TEST FOR ASSESING FILM BRITTLENESS

The coatings' brittleness and toughness can be assessed by nano-impact tests [16,17,18]. In this test, a solenoid is used to pull the indenter off the coated specimen surface and to re-accelerate it from a small distance against the film. An appropriate automation enables repetitive impacts at the same position on the sample surface at a set frequency. The evolution of the indentation depth, due to the progressing film damage during the repetitive impacts, is continuously monitored. A typical diagram illustrating the developed impact depth versus the time is shown in figure 10. The indenter geometrical characteristics are depicted in the left figure part. Moreover, based on a developed nano-impact FEM-simulation model, the film failure initiation and evolution, at various impact loads, can be determined [19]. An application of nano-impact test will be demonstrated for characterizing the brittleness of coatings after micro-blasting.

Micro-blasting on PVD films is an efficient method for improving the cutting performance of coated tools [18,20,21]. This process induces residual compressive stresses into the film structure, thus increasing the coating hardness and impairing the crack propagation, but also its brittleness [21,22,23]. In figure 11, a related characteristic example is introduced. In figure 10a, the coatings' maximum yield stresses after micro-blasting at various pressures are presented. In generally, a gradation of the yield stress versus the film thickness develops after micro-blasting [21]. The maximum yield stress and the yield to rupture stress ratio (S_Y/S_M) increase versus the micro-blasting pressure, as it is presented in figure 11b. An augmentation of this ratio indicates a simultaneous film brittleness growth i.e. coating fracture at less plastic deformation. The increase of the equivalent residual stresses is equal to the yield stress differences [24]. Considering this dependency, the equivalent residual stress changes in the coatings after

micro-blasting at various pressures were calculated and they are displayed in figure 11c. In Figure 12, nano-impact results of untreated and micro-blasted PVD TiAlN coated inserts at a pressure of 0.3 MPa are exhibited. The applied loads amount to 10 mN and 30 mN and the maximum number of impacts is equal to 1800. The maximum load of 30 mN was experimentally determined. At this load, the maximum impact depth starts increasing in the case of specimens micro-blasted at the maximum employed pressure of 0.3 MPa. One thousand eight hundred impacts were sufficient to obtain an overview concerning the imprint depth development. In the as deposited film case, increased impact loads are associated with larger imprint depths. According to the results obtained at an impact load of 10 mN, micro-blasting contributes to a significant reduction of the registered imprint depth independently by the applied number of impacts. In contrast, a different behavior is revealed at an impact load of 30 mN. In the experiment initiation i.e at the first 1000 impacts, micro-blasting results in a significant impact depth reduction compared to the corresponding one of an untreated coating. However, when the impact test is terminated, a comparable steeper depth growth occurs, caused by the coating overloading and brittleness increase at 0.3 MPa.

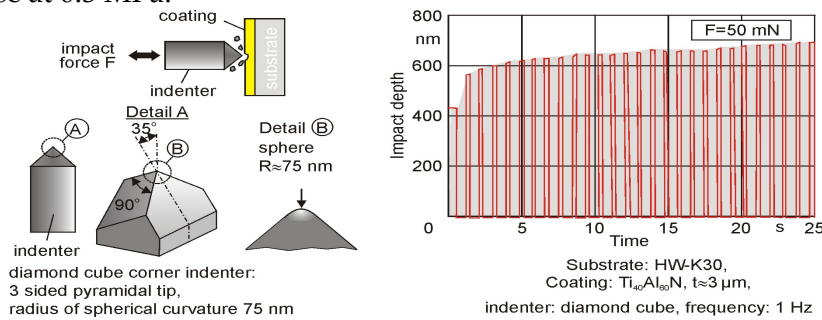


Figure 10. Characteristic nano-impact results

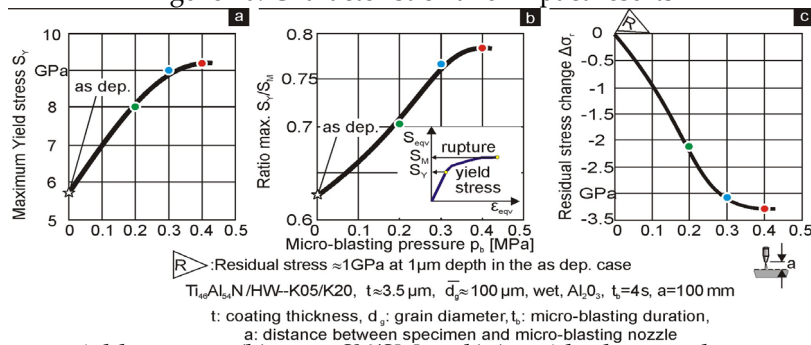


Figure 11. (a) Maximum yield stresses, (b) max. SY/SM and (c) residual stress changes ratio of micro-blasted coated inserts at various pressures.

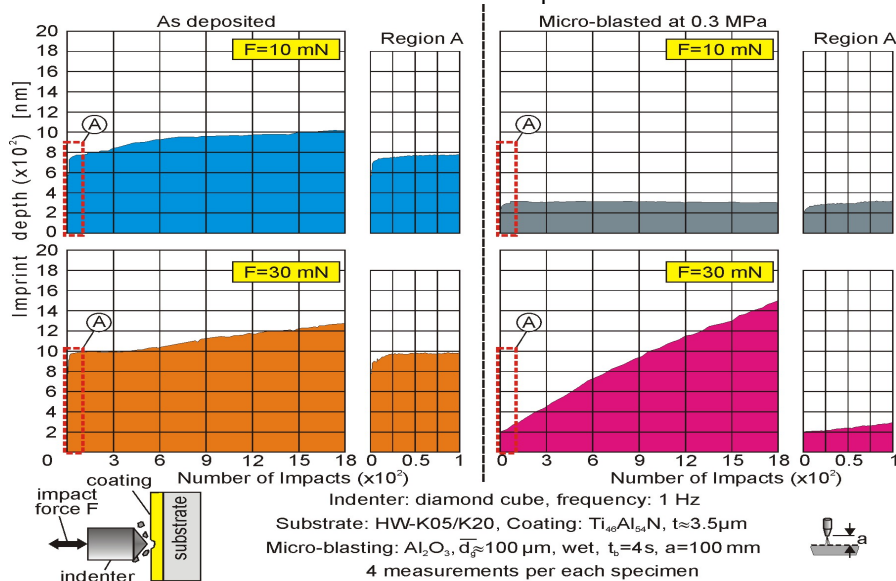


Figure 12. Characteristic nano-impact results on untreated and micro-blasted PVD films.

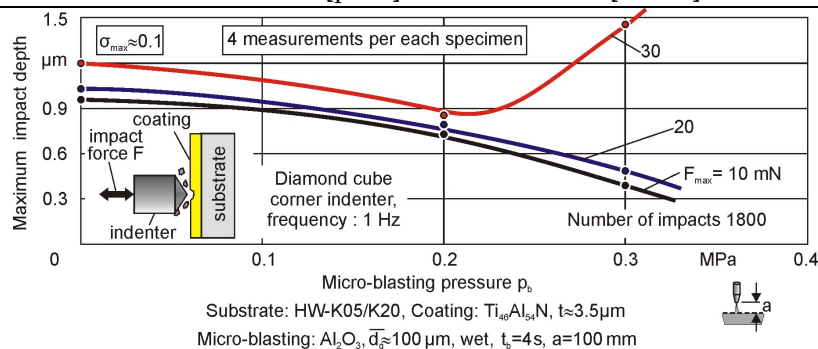


Figure 13. Nano-impact results at different impact forces on wet micro-blasted coatings at various pressures. The described in figure 11 compressive stresses increase in the film structure deteriorates the film ductility [18] and thus the coating’s brittleness grows. The nano-impact test was employed to investigate the film brittleness at various micro-blasting conditions. In the diagram of figure 13, the courses of the maximum attained impact depths at various impact loads versus the micro-blasting pressure, when coarse Al_2O_3 grains are employed, are monitored. Although up to a repetitive impact load of 20 mN, the higher micro-blasting pressure of 0.3 MPa seems to improve the film failure behaviour, at 30 mN, the increased coating brittleness leads to a larger film failure.

5. IMPACT TEST WITH MODULATED REPETITIVE FORCE FOR DETERMINING STRAIN RATE EFFECT ON THE FILM FATIGUE

Die and mold manufacturing commonly includes milling operations, which are associated with complicated cutting edge workpiece contact and intensive tool impact loads. Moreover, it has to be considered that repetitive impact loads of variable durations and amplitudes are exercised on the coated cutting edge, depending on the milling kinematics and cutting conditions. These facts render the prediction of the tool wear development difficult. Hence, it was necessary to quantify the influence of the cutting edge entry impact duration on the coated tool fatigue failure. This was enabled by a developed impact tester facilitating the impact force modulation. For rendering possible the modulation of the impact force characteristics such as of frequency, impact duration and force signal pattern, a new impact tester has been employed (see figure 14) [25]. A piezoelectric actuator is applied for the force generation. By this device, the fatigue behaviour of thin hard coatings at different impact force patterns amplitudes and durations can be investigated.

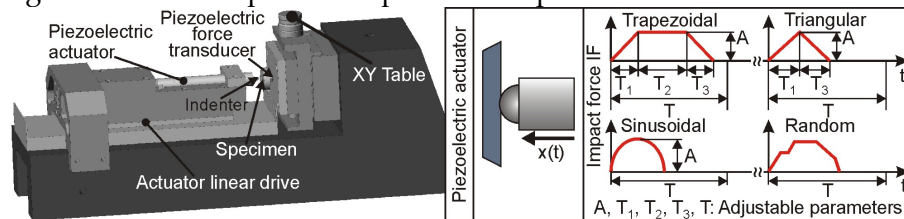


Figure 14. The employed impact tester with adjustable force signal patterns

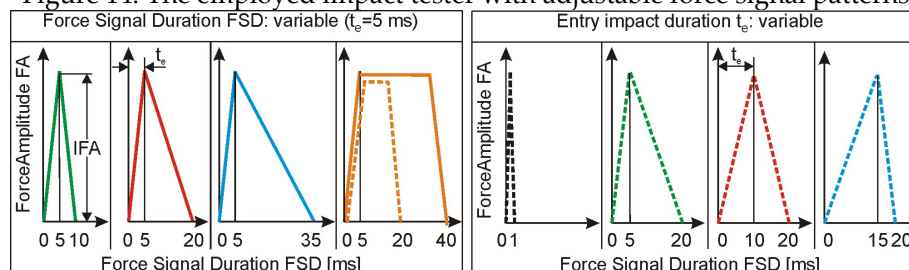


Figure 15. Triangular and trapezoidal impact force signals

For detecting the effect of the cutting edge entry impact duration on the film fatigue failure, impact tests at forces of various durations and amplitudes can be conducted (see figure 15). All applied triangular force signals with durations (FSD) of 10 ms, 20 ms and 25 ms and the trapezoidal ones of 20 ms and 40 ms, which are presented at the left figure 15 part, had a constant signal growth time t_e of 5 ms (entry impact duration t_e). In contrast, the displayed force signals at the right of

figure 15 possess different entry impact durations t_e from ca. 0.5 ms up to 15 ms. These force signals are created by the piezoelectric actuator and measured by the piezoelectric force transducer (see figure 14).

An application of the impact test with modulated force characteristics will be demonstrated for explaining the wear behaviour of coated hardmetal inserts without or with rake chamfer and additionally larger cutting edge radius in up milling hardened steel [25]. The geometry of the employed tools and the cutting inserts are shown in figure 16a. Such cutters are commonly used in NC-milling of dies and molds. Tool holders of 21 mm, 40 mm and 63 mm external diameter were employed. Based on appropriate FEM simulations, the maximum film stress course versus the cutting length of both investigated cutting edge cases are obtained (see figure 16b).

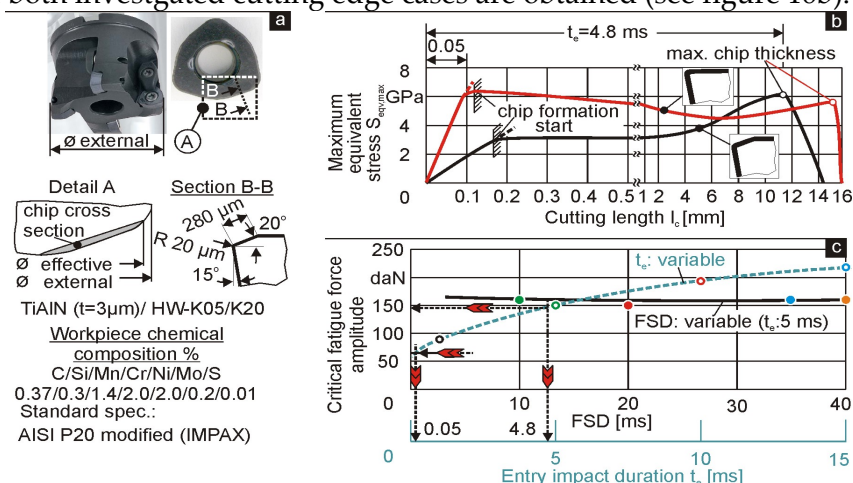


Figure 16. (a) Employed tools' and cutting inserts' geometry. (b) Developed stresses vs. the cutting length in up milling, in the cases of cutting edges with or without chamfer. (c) Effect of impact signal and entry impact durations on the critical force amplitude.

The effect of the impact force pattern on the critical force amplitude, which induces coating fatigue failure after one million impacts, is monitored in figure 16c. According to these results, the critical fatigue force amplitude remains practically invariable versus the force signal duration at constant t_e . On the other hand, t_e affects significantly the film fatigue behaviour, as it is exhibited in the same diagram. An increase of the impact entry duration t_e from 0.05 ms up to 15 ms results in a significant critical fatigue impact force amplitude augmentation from ca. 60 daN up to 220 daN respectively. The cutting load signal, i.e. the stress course versus the cutting length, when a chamfered cutting edge is used, resembles to a triangular force signal at an entry impact duration of 4.8 ms (see figure 16b). Moreover, the stress course on a cutting edge without chamfer and smaller radius, versus the cutting length corresponds to a trapezoidal force pattern at a significant lower entry impact duration of 0.05 ms. Considering these facts and the results exhibited in figure 16c, the chamfered coated cutting edges can withstand to fatigue failure approximately a two and a half times higher entry impact force amplitude. In this way, at the same stress level, the film failure of a chamfered cutting edge may appear in up milling after a longer cutting time compared to an insert without chamfer. The introduced experimental results in [25], at equal undeformed chip lengths l_{cv} , ascertain this hypothesis.

An overview of the effect of the cutting edge entry impact duration on the coated tool life is shown in figure 17. Short entry impact durations correspond to comparably reduced critical fatigue impact force amplitudes i.e. to lower coating fatigue strength. In contrast, longer entry durations improve the film fatigue behaviour and thus, they enhance the tool life. Over an entry impact duration of ca. 10 ms, the tool life at constant cutting speed and feed rate, is practically not affected by the rest cutting conditions, as for example by the undeformed chip length, tool diameter and milling kinematics.

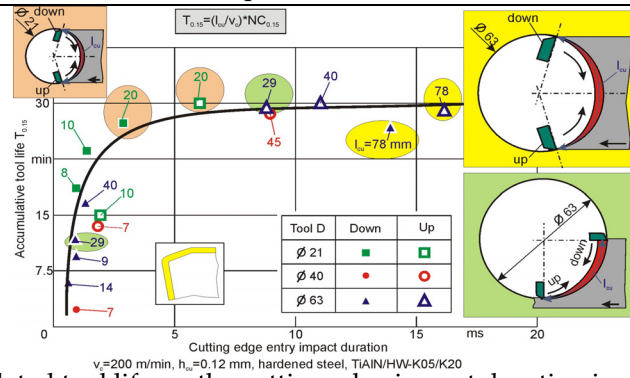


Figure 17. Accumulated tool life vs. the cutting edge impact duration in down and up milling, at various undeformed chip lengths and tool diameters

6. MICRO-BLASTING ON PVD FILMS

As it has been already described in figure 11, by micro-blasting on the coated tool surfaces, residual compressive stresses are induced into the film structure, thus leading to coating hardness and strength properties improvement. Micro-blasting parameters such as pressure, time as well as blasting grains' size and shape have a pivotal effect on the film strength properties and thus on the coated tools' cutting performance [18, 20].

Moreover, due to the film abrasion during micro-blasting, the coating thickness distributions along the cutting edge change (see figure 18). By increasing the micro-blasting pressure, an enlargement of the cutting edge radius and a simultaneous coating thickness decrease t_{pmin} develop. A coating thickness t_{pmin} diminution leads to substrate thermal and mechanical loads growth and thus, the coated tool cutting performance may be deteriorated.

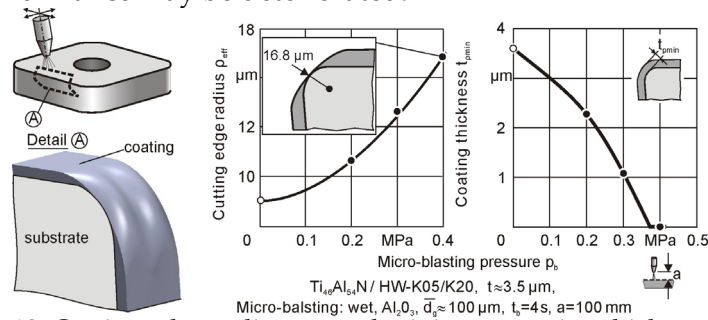


Figure 18. Cutting edge radius q_{eff} and minimum coating thickness t_{pmin} of wet micro-blasted coated inserts at various conditions.

To capture the effect of the applied micro-blasting pressure on the cutting performance of coated cemented carbide inserts, milling investigations were conducted. The applied tool-workpiece system is illustrated at the left of figure 19. In this figure, the achieved numbers of cuts, up to a flank wear land width of 0.2 mm are displayed. The cutting performance of coated micro-blasted tools at a pressure of 0.2 MPa is significantly improved compared to the corresponding performance of the untreated (as dep.) coated inserts or micro-blasted at higher than 0.2 MPa pressures.

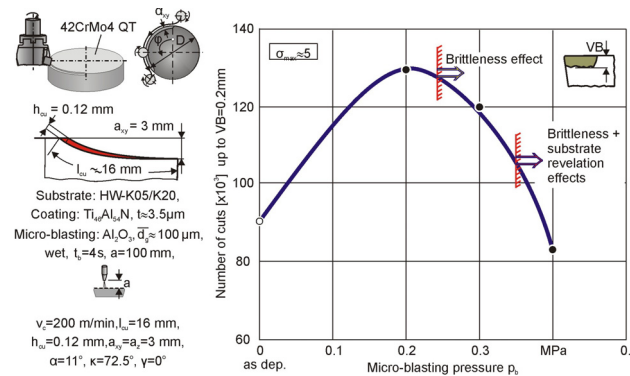


Figure 19. Cutting edge radius q_{eff} and minimum coating thickness t_{pmin} of wet micro-blasted coated inserts at various conditions

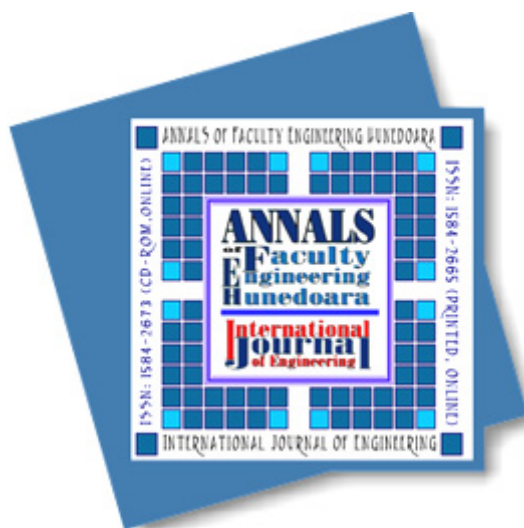
7. CONCLUSIONS

The productivity increase demands in cutting processes can be addressed, among others, through the application of coated tools. Coated tools wear mechanisms were explained by innovative methods for characterizing film material and functional properties. These issues are supported by sophisticated computational procedures, which contribute in obtaining a thorough understanding of the tool wear mechanisms taking place during cutting with coated tools. The described procedures allow the prediction of coated tool cutting performance and the effective adaption of the cutting conditions to the film properties, thus restricting the related experimental cost.

REFERENCES

- [1] Bouzakis, K.-D., Michailidis, N., Skordaris, G., Bouzakis, E., Biermann, D., M'Saoubi, R. (2012). Cutting with coated tools: Coating technologies, characterization methods and performance optimization. *CIRP Annals - Manufacturing Technology*, vol. 61, no. 2, p. 703-723.
- [2] CIRP Encyclopaedia, 2011, Coated tools.
- [3] Bouzakis, K.-D., Michailidis, N., Hadjiyiannis, S., Skordaris, G., Erkens, G. (2003). The effect of specimen roughness and indenter tip geometry on the determination accuracy of thin hard coatings stress-strain laws by nanoindentation. *Materials Characterization*, vol 49, no 2, p.149-156.
- [4] Bouzakis, K.-D., Michailidis, N., Skordaris, G. (2005). Hardness determination by means of a FEM-supported simulation of nanoindentation and applications in thin hard coatings. *Surface and Coatings Technology*, vol. 200, no. 1-4, p. 867-871.
- [5] Lucca, D.A., Herrmann, K., Klopstein, M.J. (2010). Nanoindentation: Measuring methods and applications. *CIRP Annals-Manufacturing Technology*, vol. 59, No. 2, p. 803-819.
- [6] Beake B. D., Fox-Rabinovich G. S., Veldhuis S.C., Goodes S.R. (2009). Coating optimization for high speed machining with advanced nanomechanical test methods. *Surface and Coatings Technology*, vol. 203, no. 13, p. 1919-1925.
- [7] Beake, B. D., Smith, J.F., Gray, A., Fox-Rabinovich, G.S, Veldhuis, S.C., Endrino, J.L. (2007). Investigating the correlation between nano-impact fracture resistance and hardness/modulus ratio from nanoindentation at 25–500 °C and the fracture resistance and lifetime of cutting tools with Ti1-xAlxN (x = 0.5 and 0.67) PVD coatings in milling operations. *Surface and Coatings Technology*, vol. 201, no. 8, p. 4585-4593.
- [8] Fox-Rabinovich, G.S, Beake, B. D., Endrino, J.L., Veldhuis, S.C., Parkinson, P., Shuster, L.S., Migranov, M.S. (2006). Effect of mechanical properties measured at room and elevated temperatures on the wear resistance of cutting tools with TiAlN and AlCrN coatings. *Surface and Coatings Technology*, vol. 200, no. 20-21, p.5738-5742.
- [9] Bouzakis, K.-D., Pappa, M., Skordaris, G., Bouzakis, E., Gerardis S. (2010). Correlation between PVD coating strength properties and impact resistance at ambient and elevated temperatures. *Surface and Coatings Technology*, vol. 205, no. 5, p.1481-1485.
- [10] Bouzakis, K.-D., Michailidis, N., Lontos, A., Siganos, A., Hadjiyiannis, S., Giannopoulos, G., Maliaris, G., Erkens, G. (2001). Characterization of cohesion, adhesion and creep-properties of dynamically loaded coatings through the impact tester. *Zeitschrift fuer Metallkunde/Materials Research and Advanced Techniques*, vol. 92, no. 10, p. 1180-1185.
- [11] Bouzakis, K.-D., Mirisidis, I., Michailidis, N., Lili, E., Sampris, A., Erkens, G., Cremer, R. (2007). Wear of tools coated with various PVD films: Correlation with impact test results by means of FEM simulations. *Plasma Processes and Polymers* Vol. 4, no. 3, p. 301-310.
- [12] Verein Deutscher Ingenieure Normen, VDI3198, VDI-Verlag, Duesseldorf, 1991.
- [13] Bouzakis, K.-D., Asimakopoulos, A., Skordaris, G., Pavlidou, E., Erkens, G. (2007). The inclined impact test: A novel method for the quantification of the adhesion properties of PVD films. *Wear*, vol. 262, no. 11-12, p. 1471-1478.
- [14] Klocke, F., Bouzakis, K.-D., Georgiadis, K., Gerardis, S., Skordaris, G., Pappa, M. (2011). Adhesive interlayers' effect on the entire structure strength of glass molding tools' Pt-Ir coatings by nano-tests determined. *Surface and Coatings Technology*, vol. 206, no. 7, p. 1867-1872.
- [15] Bouzakis, K.-D., Makrimalakis, S., Katirtzoglou, G., Skordaris, G., Gerardis, S., Bouzakis, E., Leyendecker, T., Bolz, S., Koelker, W. (2010). Adaption of graded Cr/CrN-interlayer thickness to cemented carbide substrates' roughness for improving the adhesion of HPPMS PVD films and the cutting performance. *Surface and Coatings Technology*, vol. 205, no. 5, p. 1564-1570.
- [16] Beake, B.D., Smith, J.F. (2004). Nano-impact testing - An effective tool for assessing the resistance of advanced wear-resistant coatings to fatigue failure and delamination. *Surface and Coatings Technology*, vol. 188-189, no. 1-3, p. 594-598.
- [17] Beake, B.D., Vishnyakov, V.M., Colligon, J.S. (2011). Nano-impact testing of TiFeN and TiFeMoN films for dynamic toughness evaluation. *Journal of Physics D: Applied Physics.*, vol. 44, no. 8: art. no. 085301.
- [18] Bouzakis, K.-D., Bouzakis, E., Skordaris, G., Makrimalakis, S., Tsouknidas, A., Katirtzoglou, G., Gerardis, S. (2011). Effect of PVD films wet micro-blasting by various Al₂O₃ grain sizes on the wear behavior of coated tools. *Surface and Coatings Technology*, vol. 205, p. S128-S132.

- [19] Bouzakis, K.-D., Gerardis, S., Skordaris, G., Bouzakis, E. (2011). Nano-impact test on a TiAlN PVD coating and correlation between experimental and FEM results. *Surface and Coatings Technology*, vol. 206, no. 7, p. 1936-1940.
- [20] Bouzakis K.-D., Klocke F., Skordaris G., Bouzakis E., Gerardis S., Katirtzoglou G., Makrimallakis S. (2011). Influence of dry micro-blasting grain quality on wear behavior of TiAlN coated tools. *Wear*, vol. 271, no. 5-6, p. 783-791.
- [21] Bouzakis, K.-D., Skordaris, Klocke, F., Bouzakis, E. (2009). A FEM-based analytical–experimental method for determining strength properties gradation in coatings after micro-blasting. *Surface and Coatings Technology*, vol. 203, no. 19, p. 2946-2953.
- [22] Barbatti, C., Garcia, J., Pitonak, R., Pinto, H., Kostka, A., Di Prinzio, A., Staia, M.H., Pyzalla, A.R. (2009). Influence of micro-blasting on the microstructure and residual stresses of CVD κ -Al₂O₃ coatings. *Surface and Coatings Technology*, vol. 203, p. 3708-3717.
- [23] Klaus, M., Genzel, Ch., Holzschuh, H. (2008). Residual stress depth profiling in complex hard coating systems by X-ray diffraction. *Thin Solid Films*, vol. 517, p. 1172-1176.
- [24] Bouzakis, K.-D., Skordaris, G., Mirisidis, J., Hadjiyiannis, S., Anastopoulos, J., Michailidis, N., Erkens, G., Cremer, R. (2003). Determination of coating residual stress alterations demonstrated in the case of annealed films and based on a FEM supported continuous simulation of the nanoindentation. *Surface and Coatings Technology*, vol. 174-175, p. 487-492.
- [25] Bouzakis, K.-D., Makrimallakis, S., Katirtzoglou, G., Bouzakis, E., Skordaris, G., Maliaris, G., Gerardis, S. (2012). Coated tools' wear description in down and up milling based on the cutting edge entry impact duration. *CIRP Annals - Manufacturing Technology*, vol. 61, no 1, p. 115-118.



ANNALS of Faculty Engineering Hunedoara – International Journal of Engineering



copyright © University Politehnica Timisoara, Faculty of Engineering Hunedoara,
5, Revolutiei, 331128, Hunedoara, ROMANIA
<http://annals.fih.upt.ro>